



Evaluations of the effective material properties of carbon nanotube-based composites using a nanoscale representative volume element

Y.J. Liu *, X.L. Chen

*Computer-Aided Engineering (CAE) Research Laboratory, Department of Mechanical Engineering, University of Cincinnati,
P.O. Box 210072, Cincinnati, OH 45221-0072, USA*

Received 15 March 2002; received in revised form 26 June 2002

Abstract

Carbon nanotubes (CNTs) possess extremely high stiffness, strength and resilience, and may provide the ultimate reinforcing materials for the development of nanocomposites. In this paper, the effective mechanical properties of CNT-based composites are evaluated using a 3-D nanoscale representative volume element (RVE) based on continuum mechanics and using the finite element method (FEM). Formulas to extract the effective material constants from solutions for the RVE under three loading cases are derived based on the elasticity theory. An extended rule of mixtures, based on the strength of materials theory for estimating the effective Young's modulus in the axial direction of the RVE, is applied for comparisons with the numerical solutions based on the elasticity theory. Numerical examples using the FEM are presented, which demonstrate that the load carrying capacities of the CNTs in a matrix are significant. With additions of the CNTs in a matrix at volume fractions of only about 2% and 5%, the stiffness of the composite can increase as many as 0.7 and 9.7 times for the short and long CNT cases, respectively. These simulation results are consistent with the experimental ones reported in the literature.

© 2002 Elsevier Science Ltd. All rights reserved.

Keywords: Carbon nanotubes; Nanocomposites; Effective properties; Finite element method

1. Introduction

There has been great interest in recent years in nanocomposites based on nanotubes or nanoparticles. Carbon nanotubes (CNTs), discovered by Iijima in 1991 (Iijima, 1991), possess exceptionally high stiffness, strength and resilience, as well as

superior electrical and thermal properties. Many believe that CNTs may provide the ultimate reinforcing materials for the development of a new class of nanocomposites (see, e.g. Qian et al., 2002; Thostenson et al., 2001). It has been demonstrated that with only 1% (by weight) of CNTs added in a matrix material, the stiffness of a resulting composite film can increase between 36% and 42% and the tensile strength by 25% (Qian et al., 2000). The mechanical-load carrying capacities of CNTs in nanocomposites have also been demonstrated in some experimental work (Schadler et al., 1998;

* Corresponding author. Tel.: +1-513-556-4607; fax: +1-513-556-3390.

E-mail address: yijun.liu@uc.edu (Y.J. Liu).

Wagner et al., 1998; Bower et al., 1999; Qian et al., 2000) and simulations (Liu and Chen, 2002). All these studies show that the CNT-based composites have the potential to provide extremely strong and ultra light new materials. However, enormous challenges remain in the development of such nanocomposites. Currently, fabrication of CNT-based composites is still a difficult and expensive process. Many basic issues ranging, for example, from characterizations, experimental techniques to simulation methods, have not been fully addressed for the development of CNT-based composites.

Computational approach can play a significant role in the development of the CNT-based composites by providing simulation results to help on the understanding, analysis and design of such nanocomposites. At the nanoscale, analytical models are difficult to establish or too complicated to solve, and tests are extremely difficult and expensive to conduct. Modeling and simulations of nanocomposites, on the other hand, can be achieved readily and cost effectively on even a desktop computer. Characterizing the mechanical properties of CNT-based composites is just one of the many important and urgent tasks that simulations can accomplish.

In this paper, the effective mechanical properties of CNT-based composites are evaluated using a 3-D nanoscale representative volume element (RVE) based on continuum mechanics and using the finite element method (FEM). Selections of the RVEs are discussed in Section 2. Formulas based on the elasticity theory to extract the material constants from numerical analysis are derived in Section 3. Analytical results based on the strength of materials theory to estimate Young's modulus in the axial direction and to help validate the numerical solutions are summarized in Section 4. Numerical examples using the FEM are presented in Section 5. Finally, some discussions and conclusions are offered in Section 6.

2. RVEs for evaluations of the effective material properties

Simulations of *individual* CNTs using atomistic or molecular dynamics (MD) models have pro-

vided abundant results for the understanding of mechanical and electrical behaviors of the CNTs (Cornwell and Wille, 1997; Han et al., 1997; Gao et al., 1998; Halicioglu, 1998; Sinnott et al., 1998; Buongiorno Nardelli et al., 2000; Kang and Hwang, 2001; Macucci et al., 2001; Srivastava et al., 2001). However, these atomistic or MD simulations are currently limited to very small length and time scales and cannot deal with the larger length scales in nanocomposites, due to the limitations of current computing power (for example, a $1 \times 1 \times 1 \mu\text{m}^3$ cube could contain up to 10^{12} atoms). Nanocomposites for engineering applications expand from nano to micro, and eventually to macro length scales, which must be addressed by other simulation approaches or combinations of MD with other approaches.

Continuum approaches based on continuum mechanics have also been applied successfully for simulating the mechanical responses of *individual* or *isolated* carbon nanotubes which are treated as beams, thin shells or solids in cylindrical shapes (Wong et al., 1997; Sohlberg et al., 1998; Govindjee and Sackman, 1999; Ru, 2000; Qian et al., 2001; Qian et al., 2002; Ru, 2001). These studies suggest that the continuum mechanics approach can be applied safely to investigate the mechanical behaviors of the CNTs when the lengths of the CNTs are about 100 nm and above. For example, in (Wong et al., 1997), the authors successfully applied the simple beam theory to model CNTs and extracted Young's modulus of the CNT from the force–deflection curve obtained from their experiment. Their results are consistent with other reported work. Although successful to some extent and efficient in computation for models at larger length scales, continuum mechanics at this threshold faces the risk of breakdowns more than ever before, compared with the micromechanics simulations. The preferred approach for simulations of CNT-based composites should be a multiscale one where the MD and continuum mechanics are integrated in a computing environment that is detailed enough to account for the physics at nanoscales while efficient enough to handle nanocomposites at larger length scales.

Before a multiscale approach for simulations of nanocomposites is successfully developed, the

continuum mechanics approach seems to be the only feasible approach now for conducting some preliminary studies of such materials. A study of the CNTs *in a matrix* was given in a recent paper (Liu and Chen, 2002) in which the interactions of the CNT with the matrix, interfacial stresses and load-carrying capabilities of the CNTs are investigated based on 3-D elasticity models. It is proposed in (Liu and Chen, 2002) that the 3-D elasticity models, instead of beam or shell models, should be used for the CNTs, as well as the matrix, in order to ensure the accuracy and compatibility of the models for the CNTs and the matrix. One way to develop manageable 3-D continuum models for the study of CNT-based composites is to extend the concept of representative volume elements used for conventional fiber-reinforced composites at the microscale (Hyer, 1998; Nemat-Nasser and Hori, 1999).

CNTs are in different sizes and forms when they are dispersed in a matrix to make a nanocomposite. They can be single-walled or multi-walled with length of a few nanometers or a few micrometers, and can be straight, twisted and curled, or in the form of ropes (Schadler et al., 1998; Wagner et al., 1998; Bower et al., 1999; Qian et al., 2000; Qian et al., 2001; Thostenson et al., 2001). Their distribution and orientation in the matrix can be uniform and unidirectional (which may be the ultimate goal) or random. All these factors make the simulations of CNT-based composites extremely difficult. To start with, the concept of unit cells or representative volume elements, which have been applied successfully in the studies of conventional fiber-reinforced composites at the microscale (Hyer, 1998; Nemat-Nasser and Hori, 1999) can be extended to study the CNT-based composites at the nanoscale. In this RVE approach, a single (or multiple) nanotube(s) with surrounding matrix material can be modeled, with properly applied boundary and interface conditions to account for the effects of the surrounding materials. Numerical methods, such as the FEM, boundary element method (Liu et al., 2000; Chen and Liu, 2001) or meshfree method (Qian et al., 2001) can be applied to analyze the mechanical responses of these RVEs under different loading conditions.

Interfaces between the CNTs and matrix are crucial regions to ensure the load carrying capacity and other functionalities of the nanocomposites. They are also the most difficult regions for any simulation approaches. To start with, *perfect bonding* can be assumed between the CNTs and matrix in the continuum mechanics models of CNT-based composites. Research has demonstrated that the possibility of such a strong (C–C) bond exists for CNT-based composites (Jia et al., 1999; Thostenson et al., 2001). For a “less” perfect bond, a *spring-like* model can be used between the CNTs and matrix. A thin *interphase* model (e.g., a thin coating on the CNTs) can also be introduced to account for a third phase between the CNTs and matrix. The properties of this interphase region can be used to characterize the interface properties. Other interface models, such as *friction* models considering the slip/stick along a CNT/matrix interface or a *van der Waals* type of models (for multi-walled CNTs (Ru, 2000; Qian et al., 2002)) can certainly be developed for modeling CNT-based composites, with improved understanding based on further nanoscale experiments and MD simulations. In this paper, only the perfect bonding between the CNT and the matrix in RVE models is considered.

Three *nanoscale* representative volume elements (Fig. 1) based on the 3-D elasticity theory have been proposed in (Liu and Chen, 2002) for the study of CNT-based composites. They are the cylindrical RVE (Fig. 1(a)), square RVE (Fig. 1(b)) and hexagonal RVE (Fig. 1(c)). The cylindrical RVE can be applied to model the CNTs which have different diameters (Hyer, 1998) or CNTs embedded in a regular carbon fiber. Under axisymmetric as well as antisymmetric loading, a 2-D axisymmetric model can be applied for the cylindrical RVE, which can significantly reduce the computational work (Liu and Chen, 2002). Similar to the study of conventional fiber-reinforced composites (Hyer, 1998), the square RVE models can be applied when the CNTs are arranged evenly in a square array, while the hexagonal RVE models can be applied when CNTs are in a hexagonal array, in the transverse direction. These RVEs can be used to study the interactions of a CNT with the matrix, such as the load transfer

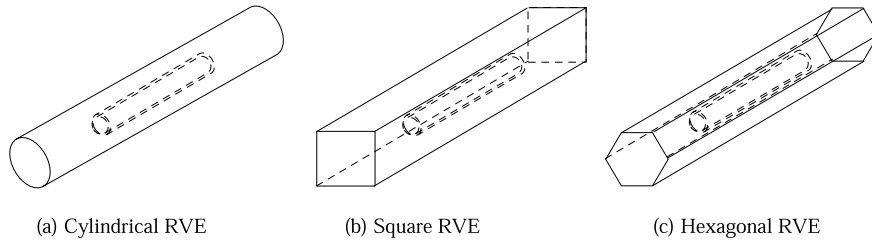


Fig. 1. Three nanoscale representative volume elements for the analysis of CNT-based nanocomposites.

mechanism and stress distributions along the interfaces (Liu and Chen, 2002) or to evaluate the effective material properties of the CNT-based composites, which is the focus of this current paper.

To start with, the *cylindrical RVE* will be employed first in this paper to evaluate the effective Young's moduli and Poisson's ratios of the CNT-based composites. The required mathematical results to be used to extract these material constants from the simulation results (by using either the FEM or other methods) will be established in the next section.

3. Formulas for evaluations of the effective material constants

It is assumed that both the CNTs and matrix in a RVE are continua of linearly elastic, isotropic and homogenous materials, with given Young's moduli and Poisson's ratios. It is also assumed that the CNTs and matrix are perfectly bonded at the interface in the RVE to be studied. Other material models and interface conditions (Liu and Chen, 2002) can certainly be considered in more sophisticated investigations. The RVE can contain one CNT (Fig. 2) or multiple CNTs, determined by the main criterion that it should be large enough to be representative of the material and small enough to be modeled and analyzed efficiently using a solution method. Under the above assumptions, there will be four effective material constants to be determined for the CNT-based composite, namely, two Young's moduli $E_x (=E_y)$ and E_z , and two Poisson's ratios ν_{xy} and $\nu_{zx} (= \nu_{zy})$ (see Fig. 2 for the orientation of the coordinates).

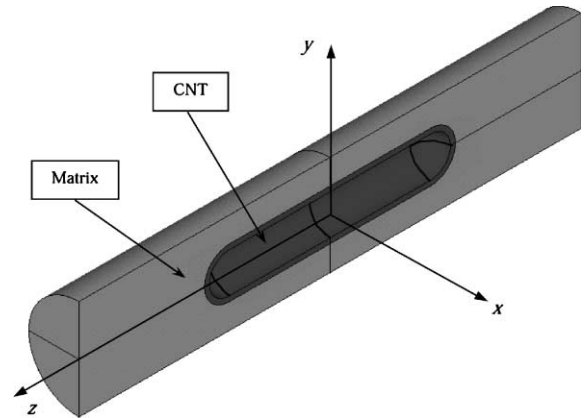


Fig. 2. A cylindrical RVE shown in a cut-through view.

To derive the formulas for extracting the four material constants, a homogenized elasticity model corresponding to the RVE is considered. The geometry of the elasticity model is corresponding to a hollow cylindrical RVE with length L , inner radius r_i and outer radius R (Fig. 3), so that analytical solutions can be obtained. This geometry can account for the cases when the CNT is relatively long and thus all the way through the length of the RVE. In the case that the CNT is relatively short and thus fully inside the RVE, a solid cylindrical RVE ($r_i = 0$) can be used for extracting the material constants, since the elasticity solutions are difficult to find in this case. The elasticity model has a single material with the four effective material constants (E_x , E_z , ν_{xy} and ν_{zx}) to be determined.

The material of the elasticity model is *transversely isotropic* and the general 3-D strain–stress relations are given by (see, e.g. (Hyer, 1998))

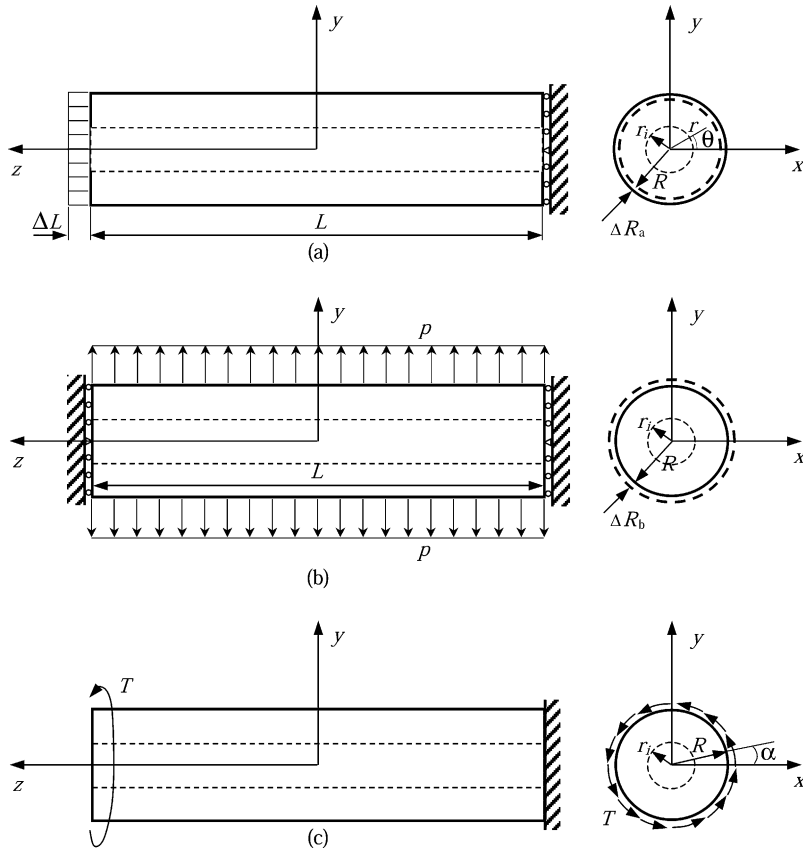


Fig. 3. Three loading cases for the cylindrical RVE used to evaluate the effective material properties of the CNT-based composites. (a) Under axial stretch ΔL ; (b) Under lateral uniform load P ; (c) Under torsional load T .

$$\begin{Bmatrix} \varepsilon_x \\ \varepsilon_y \\ \varepsilon_z \end{Bmatrix} = \begin{bmatrix} \frac{1}{E_x} & -\frac{\nu_{xy}}{E_x} & -\frac{\nu_{zx}}{E_z} \\ -\frac{\nu_{xy}}{E_x} & \frac{1}{E_x} & -\frac{\nu_{zx}}{E_z} \\ -\frac{\nu_{zx}}{E_z} & -\frac{\nu_{zx}}{E_z} & \frac{1}{E_z} \end{bmatrix} \begin{Bmatrix} \sigma_x \\ \sigma_y \\ \sigma_z \end{Bmatrix}, \quad (1)$$

in the (x, y, z) coordinates shown in Fig. 2. This relation is also valid for the stress and strain components in the cylindrical coordinate system (r, θ, z) (Fig. 3(a)). To determine the four unknown material constants, four equations based on the elasticity theory will be needed. Three loading cases (Fig. 3) have been devised as illustrated in the following subsections to provide four such equations. Note that for transversely isotropic materials, the other material constants are related to the four constants $(E_x, E_z, \nu_{xy}, \nu_{zx})$ used in Eq. (1). For example,

$$E_y = E_x, \quad \nu_{yx} = \nu_{xy}, \quad \nu_{zy} = \nu_{zx}, \quad \text{and} \\ \nu_{yz} = \nu_{zx} = \frac{E_x}{E_z} \nu_{zx}.$$

3.1. Cylindrical RVE under an axial stretch ΔL (Fig. 3(a))

In this load case (Fig. 3(a)), the stress and strain components at any point on the lateral surface are

$$\sigma_x = \sigma_y = \sigma_r = \sigma_\theta = 0, \quad \varepsilon_z = \frac{\Delta L}{L},$$

$$\varepsilon_\theta = \frac{\Delta R_a}{R}, \quad \text{with } \Delta R_a < 0, \quad \text{if } \Delta L > 0,$$

where ΔR_a is the radial displacement, and r and θ indicate the radial and tangential components in

the polar coordinate system, respectively. From the third equation in (1), one has immediately

$$E_z = \frac{\sigma_z}{\varepsilon_z} = \frac{L}{\Delta L} \sigma_{\text{ave}}, \quad (2)$$

where the averaged stress is given by

$$\sigma_{\text{ave}} = \frac{1}{A} \int_A \sigma_z(x, y, L/2) dx dy,$$

with A being the area of the end surface. σ_{ave} can be evaluated for the RVE using the FEM results.

Also, from Eq. (1) (applied in the cylindrical coordinate system) and the above results, one has

$$\varepsilon_\theta = -\frac{v_{zx}}{E_z} \sigma_z = -v_{zx} \frac{\Delta L}{L} = \frac{\Delta R_a}{R}.$$

Thus, one obtains

$$v_{zx} = -\left(\frac{\Delta R_a}{R}\right) / \left(\frac{\Delta L}{L}\right). \quad (3)$$

Eqs. (2) and (3) can be applied to estimate the effective Young's modulus E_z and Poisson's ratio v_{zx} ($= v_{zy}$), once the contraction ΔR_a and the stress σ_{ave} in load case (a) are obtained.

3.2. Cylindrical RVE under a lateral uniform load p (Fig. 3(b))

In this load case (Fig. 3(b)), the RVE is constrained in the z -direction so that the plane strain condition is maintained, in order to simulate the interactions of the RVE with surrounding materials in the z -direction. The RVE is loaded with a uniformly distributed load (negative pressure) p in the lateral (radial) direction. This is an axisymmetric case for both the geometry and loading. For the corresponding elasticity model (Fig. 3(b)), one has the following results for the stress and strain components at a point on the lateral surface (Timoshenko and Goodier, 1987):

$$\sigma_r = p, \quad \sigma_\theta = \frac{R^2 + r_i^2}{R^2 - r_i^2} p, \quad \text{and} \quad \varepsilon_\theta = \frac{\Delta R_b}{R},$$

where ΔR_b is the radial displacement in this load case. Applying the stress–strain relation derived from (1) for the plane strain case ($\varepsilon_z = 0$, $\sigma_z = v_{zx}(\sigma_r + \sigma_\theta)$), one has, on the lateral surface:

$$\begin{aligned} \varepsilon_\theta &= -\left(\frac{v_{xy}}{E_x} + \frac{v_{zx}^2}{E_z}\right) \sigma_r + \left(\frac{1}{E_x} - \frac{v_{zx}^2}{E_z}\right) \sigma_\theta \\ &= \left[-\left(\frac{v_{xy}}{E_x} + \frac{v_{zx}^2}{E_z}\right) + \left(\frac{1}{E_x} - \frac{v_{zx}^2}{E_z}\right) \frac{R^2 + r_i^2}{R^2 - r_i^2}\right] p \\ &= \frac{\Delta R_b}{R}. \end{aligned}$$

The first equation for determining E_x and v_{xy} is therefore found to be

$$-\left(\frac{v_{xy}}{E_x} + \frac{v_{zx}^2}{E_z}\right) + \left(\frac{1}{E_x} - \frac{v_{zx}^2}{E_z}\right) \frac{R^2 + r_i^2}{R^2 - r_i^2} = \frac{\Delta R_b}{pR}, \quad (4)$$

in which E_z and v_{zx} are assumed to have been determined from Eqs. (2) and (3).

3.3. Cylindrical RVE under a torsional load T (Fig. 3(c))

Under the applied torque T (Fig. 3(c)), which is an antisymmetric load on an axisymmetric model, the rotation angle of the left end of the RVE is given by (Timoshenko and Goodier, 1987)

$$\alpha = \frac{TL}{G_{xy}J}, \quad \text{with} \quad G_{xy} = \frac{E_x}{2(1 + v_{xy})}, \quad \text{and}$$

$$J = \pi(R^4 - r_i^4)/2,$$

where G_{xy} is the shear modulus (in the xy plane) and J the polar moment of inertia of the annular cross sectional area. Thus, one obtains the second equation:

$$\frac{E_x}{2(1 + v_{xy})} = G_{xy} \left(= \frac{TL}{\alpha J} \right). \quad (5)$$

By solving Eqs. (4) and (5), one obtains the effective Young's modulus and Poisson's ratio in the transverse direction (xy plane):

$$\begin{aligned} E_x = E_y &= 2(1 + v_{xy})G_{xy} \\ &= \frac{4pR^3 E_z G_{xy}}{pRE_z(R^2 - r_i^2) + 2E_z G_{xy}(R^2 - r_i^2)\Delta R_b + 4pR^3 v_{zx}^2 G_{xy}}, \end{aligned} \quad (6)$$

$$v_{xy} = -1$$

$$+ \frac{2pR^3 E_z}{pRE_z(R^2 - r_i^2) + 2E_z G_{xy}(R^2 - r_i^2)\Delta R_b + 4pR^3 v_{zx}^2 G_{xy}}, \quad (7)$$

where $G_{xy} = TL/\alpha J$ is determined from the rotation angle α .

When the CNTs are relatively short and thus fully inside the RVE or the radii of the CNTs are small, as an approximation, one can use a solid cylinder RVE and apply the following simplified equations obtained by setting $r_i = 0$ in Eqs. (6) and (7):

$$E_x = E_y = \frac{4pR^3 E_z G_{xy}}{pR^3 E_z + 2E_z G_{xy} R^2 \Delta R_b + 4pR^3 v_{zx}^2 G_{xy}}, \quad (8)$$

$$v_{xy} = -1 + \frac{2pR^3 E_z}{pR^3 E_z + 2E_z G_{xy} R^2 \Delta R_b + 4pR^3 v_{zx}^2 G_{xy}}. \quad (9)$$

Once the radial displacement ΔR_b in case (b) and the rotation angle α in case (c) are determined from, for example, a finite element analysis of the RVE, the effective Young’s modulus E_x and Poisson’s ratio v_{xy} can be evaluated by using Eqs. (6) and (7) for RVEs with long CNTs or Eqs. (8) and (9) for RVEs with short CNTs.

4. Analytical results based on the strength of materials theory

Some simple analytical expressions, or rules of mixtures, based on the strength of materials theory for estimating the effective Young’s modulus E_z in the axial direction of the cylindrical RVEs are summarized in this section for the convenience of comparison. These expressions can be applied to validate the numerical results using the FEM and based on the elasticity formulas obtained in the previous section. Although the strength of materials theory is not accurate for stress, especially interfacial stress, evaluations, it is fairly accurate and efficient in predicting the effective material constants in the axial direction of the RVEs, which are basically dependent on the overall responses of the RVEs. Extended coverage of these results in more general cases can be found in (Nemat-Nasser and Hori, 1999; Hyer, 1998).

4.1. CNT through the length of the RVE (Fig. 4(a))

This is the case when the CNT is relatively long (with large aspect ratio) and therefore a segment

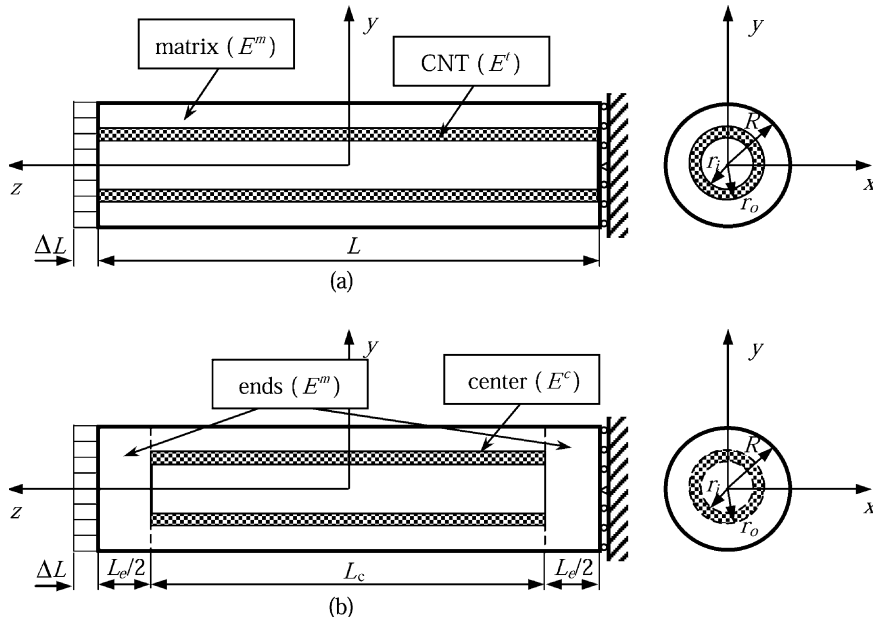


Fig. 4. Simplified strength of materials models used to derive the analytical expressions for the effective Young’s modulus E_z .

can be modeled using an RVE. The volume fraction of the CNT (a tube, Fig. 4(a)) is

$$V^t = \frac{\pi(r_o^2 - r_i^2)}{\pi(R^2 - r_i^2)} = \frac{r_o^2 - r_i^2}{R^2 - r_i^2}. \quad (10)$$

Apply the strength of materials theory and assume the matrix and CNT deform independently of each other under the stretch ΔL (Fig. 4(a)). By considering the compatibility of strains and equilibrium of stresses, one obtains the following expression for the effective Young's modulus in the axial direction:

$$E_z = E^t V^t + E^m (1 - V^t), \quad (11)$$

where E^m and E^t are the Young's modulus of the matrix and CNT, respectively. This is the same *rule of mixtures* as applied for predicting the effective Young's modulus in the fiber direction for conventional fiber-reinforced composites and is a close approximation of or identical (if the matrix and fiber have the same Poisson's ratio) to the elasticity solution (Hyer, 1998; Nemat-Nasser and Hori, 1999).

4.2. CNT inside the RVE (Fig. 4(b))

In this case (Fig. 4(b)), the RVE can be divided into two segments: one segment accounting for the two ends with total length L_c and Young's modulus E^m ; and another segment accounting for the center part with length L_c and an *effective* Young's modulus E^c . Note that the two hemispherical end caps of the CNT have been ignored in this derivation. Since the center part is a special case of Fig. 4(a), its effective Young's modulus is found to be

$$E^c = E^t V^t + E^m (1 - V^t), \quad (12)$$

using Eq. (11), in which the volume fraction of the CNT V^t given by Eq. (10) is computed based on the center part of the RVE (with length L_c) only.

Again, by considering the compatibility of strains and equilibrium of stresses, one obtains the following expression for the effective Young's modulus in the axial direction:

$$E_z = \left[\frac{1}{E^m} \left(\frac{L_c}{L} \right) + \frac{1}{E^c} \left(\frac{L_c}{L} \right) \left(\frac{A}{A_c} \right) \right]^{-1} \quad (13)$$

or in a more symmetric form:

$$\frac{1}{E_z} = \frac{1}{E^m} \left(\frac{L_c}{L} \right) + \frac{1}{E^c} \left(\frac{L_c}{L} \right) \left(\frac{A}{A_c} \right), \quad (14)$$

in which the areas $A = \pi R^2$ and $A_c = \pi(R^2 - r_i^2)$. Eq. (13) or Eq. (14) can be viewed as an *extended rule of mixtures* compared to that given in Eq. (11), and can be employed to estimate the effective Young's modulus for the case shown in Fig. 4(b) when the CNT is inside the RVE. Eq. (13) is also a more general result, as the result in Eq. (11) for the case of the RVE shown in Fig. 4(a) can be recovered from Eq. (13).

As an example, consider an RVE of a CNT in a matrix with the following dimensions:

$$L = 100 \text{ nm}, \quad L_c = L_c = 50 \text{ nm},$$

$$R = 10 \text{ nm}, \quad r_o = 5 \text{ nm},$$

$$r_i = 4.6 \text{ nm (CNT thickness} = 0.4 \text{ nm)}, \quad \text{and}$$

$$E^t = 5E^m.$$

One calculates from (10), (12) and (13)

$$V^t = 0.04871, \quad E^c = 1.1948E^m \quad \text{and}$$

$$E_z = 0.9701E^m,$$

which yields a lower effective Young's modulus for the composite, compared with that of the matrix, with the given geometry. This may suggest that the moderate increase of the stiffness of the CNT can not compensate the loss of the material caused by the hollow CNT. However, with the same dimensions, if one has

$$E^t = 10E^m, \quad \text{then } E^c = 1.4384E^m \quad \text{and}$$

$$E_z = 1.0628E^m,$$

which is a 6.28% increase for the effective modulus. Furthermore, if the CNT has a length equal to that of the RVE (Fig. 4(a), or $L_c = 0$, $L_c = L = 100$ nm), one has $E_z = E^c = 1.4384E^m$, which is a 43.84% increase for the effective Young's modulus of the composite.

More parametric studies using Eqs. (11) and (13) can be performed to obtain quick estimates of the Young's modulus in the axial direction of a CNT-based composite with different sizes and material combinations. Eqs. (11) and (13) are also directly applicable or easily extendible to cases

when the RVE contains more than one CNTs or the RVE has a square or hexagonal cross section (Fig. 1). In this paper, Eqs. (11) and (13) will be applied in the next section to verify the FEM estimates of the effective Young's moduli in the axial direction based on the elasticity results established in the previous section.

5. Numerical results

To evaluate the effective material constants of a CNT-based nanocomposite, the cylindrical RVE (Fig. 2) for a single-walled carbon nanotube in a matrix material is studied using the finite element method. The deformations and stresses are computed first for the three loading cases (Fig. 3) described in Section 3. The FEM results are then processed, and Eqs. (2), (3), (6)–(9) are applied to extract the effective Young's moduli and Poisson's ratios for the CNT-based composite. Two examples are studied, one on an RVE with a long CNT and the other on an RVE of the same size but with a short CNT.

In all the cases, axisymmetric FEM models are used since the RVEs have an axisymmetric geometry and all the three loading cases (Fig. 3) to be analyzed are either axisymmetric (Fig. 3(a), (b)) or antisymmetric (Fig. 3(c)), both of which can be handled by axisymmetric FEM models. Quadratic (8-node) ring elements for axisymmetric problems are employed, which are second order elements and offer better accuracy in stress analysis.

5.1. A long CNT through the RVE

First, an RVE for a long CNT all the way through the RVE length, similar to the one shown in Fig. 4(a), is studied. The dimensions are: for matrix, length $L = 100$ nm, radius $R = 10$ nm; for CNT, length $L = 100$ nm, outer radius $r_o = 5$ nm, inner radius $r_i = 4.6$ nm (effective thickness = 0.4 nm). The Young's moduli and Poisson's ratios used for the CNT and matrix are:

$$\begin{aligned} \text{CNT:} \quad & E^t = 1000 \text{ nN/nm}^2 \text{ (GPa)}, \quad \nu^t = 0.3; \\ \text{Matrix:} \quad & E^m = 5, 20, 100 \text{ and } 200 \text{ nN/nm}^2 \text{ (GPa)}, \\ & \nu^m = 0.3; \end{aligned}$$

where the values of the Young's modulus for the matrix are representative of that of a polymer to that of a steel. The values of the dimensions and material constants are chosen within the wide ranges of those for CNTs as reported in the literature (Ruoff and Lorents, 1995; Treacy et al., 1996; Cornwell and Wille, 1997; Lu, 1997; Wong et al., 1997; Gao et al., 1998; Krishnan et al., 1998; Yao and Lordi, 1998; Goze et al., 1999; Salvétat et al., 1999; Buongiorno Nardelli et al., 2000) and can be modified or fine-tuned readily for a specific case in future simulations.

The finite element mesh used is shown in Fig. 5(a). One layer of elements are used for the CNT in this mesh which is found to be fine enough to deliver converged FEM results. Small elements comparable in sizes to those for the CNT are also needed in the matrix surrounding the CNT to ensure the connectivity and to avoid elements with large aspect ratios. The FEM model is loaded with the three load cases shown in Fig. 3. The four material constants are extracted from Eqs. (2), (3), (6) and (7) using the FEM results.

The FEM results for the effective material constants of the CNT-composite studied are listed in Table 1. The strength of materials solutions for the effective Young's modulus E_z is also listed in Table 1 for comparison. The strength of materials solutions (Eq. (11)) are identical to those using the FEM, due to the simple geometry and load condition in this example. The results reveal that the increase of the stiffness of the composite can be significant, especially in the CNT axial direction. With the volume fraction of the CNT being at only about 5%, the stiffness of the composite in the axial direction (E_z) can increase by more than nine times compared with that of the matrix, when $E^t/E^m = 200$ (CNTs in a polymer matrix). The increases of the stiffness in the transverse direction (E_x) are also remarkable, from about 17% to 2.8 times when the ratio E^t/E^m changes from 5 to 200, in this long CNT case.

5.2. A short CNT inside the RVE

Next, an RVE for a short CNT in a matrix, as shown in Fig. 2, is studied. All the dimensions for

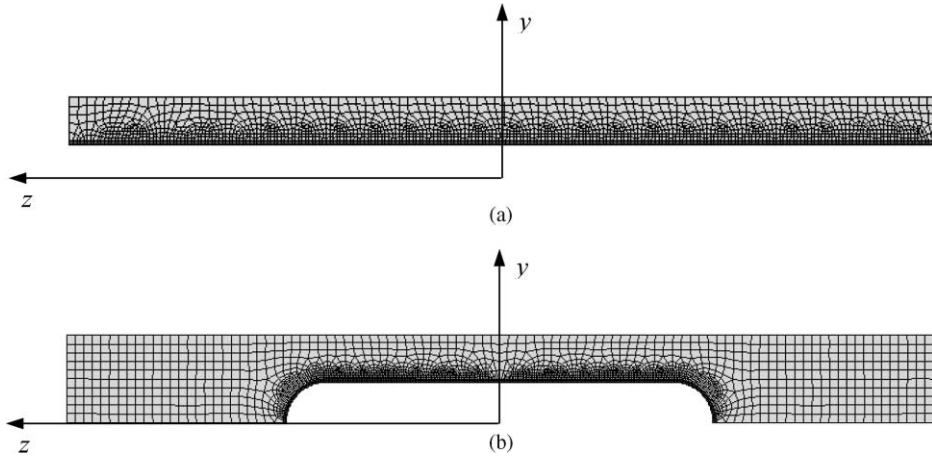


Fig. 5. Axisymmetric FEM models for the RVEs (CNT thickness = 0.4 nm). (a) CNT through the RVE (one layer of elements for the CNT, 6413 nodes); (b) CNT inside the RVE (two layers of elements for the CNT, 9296 nodes).

Table 1
Computed effective material constants for Case (a): CNT through the RVE

E^t/E^m	E_z/E^m		$E_x/E^m, E_y/E^m$	ν_{xy}	ν_{zx}, ν_{zy}
	FEM	Eq. (11)			
5	1.1948	1.1948	1.1737	0.4204	0.3000
10	1.4384	1.4384	1.3336	0.4855	0.3000
50	3.3866	3.3866	2.1502	0.4640	0.3000
200	10.6925	10.6925	3.7654	0.0431	0.3000

Note: CNT modulus $E^t = 1000$ GPa, thickness = 0.4 nm, volume fraction = 0.04871.

the RVE are the same as in the previous example, except for the CNT total length, which is reduced to 50 nm (with the two hemispherical end caps). The material constants used for the CNT and matrix are the same as in the first example. The finite element mesh used is shown in Fig. 5(b). Two layers of elements are used through the thickness of the CNT due to the increased complexity in the geometry. Coupled DOF constraint is imposed for the lateral surface under the axial load so that all points on the surface will move the same amount

in the radial direction to simulate the constraints from the surrounding material.

A stress contour plot of the first principal stresses in the RVE under the axial stretch is shown in Fig. 6. The load-carrying capacity of the CNT is obvious. More stress analysis results for CNTs interacting with a matrix material can be found in Ref. (Liu and Chen, 2002). The computed four effective material constants using the FEM results for the RVE under the three loading cases (Fig. 3) are shown in Table 2, along with the

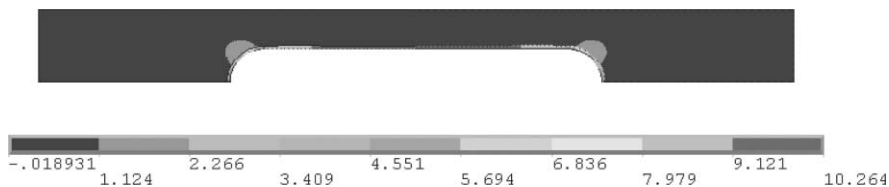


Fig. 6. Plot of the first principal stresses for the short CNT model under the axial stretch ($E^t/E^m = 10$).

Table 2
Computed effective material constants for Case (b): CNT inside the RVE

E^t/E^m	E_z/E^m		FEM		
	FEM	Eq. (13)	$E_x/E^m, E_y/E^m$	ν_{xy}	ν_{xz}, ν_{zy}
5	0.9665	0.9701	0.9541	0.2304	0.2987
10	1.0491	1.0628	1.0033	0.2614	0.3014
50	1.3925	1.4550	1.1608	0.3055	0.2925
200	1.6920	1.7879	1.2878	0.3043	0.2758

Note: CNT modulus $E^t = 1000$ GPa, thickness = 0.4 nm, volume fraction = 0.0211.

strength of materials solutions (Eq. (13)) for the stiffness in the axial direction (E_z). The increases of the stiffness in both axial and lateral directions are moderate for $E^t/E^m = 10, 50$ and 200, due to the small volume fraction of the CNT (about 2%). At $E^t/E^m = 5$, the two stiffness are actually dropped due to the reason explained earlier (the increase of the stiffness in the CNT can not compensate the loss of the material due to the reduced volume). All these results suggest that short CNTs in a matrix may not be as effective as long CNTs in reinforcing the composites.

The strength of materials solutions for the stiffness in the axial direction (E_z), using the *extended rule of mixtures* (Fig. 4(b) and Eq. (13)), are quite close to the FEM solutions which are based on 3-D elasticity, with the largest differences less than 6%. Therefore, the extended rule of mixtures (Eq. (13)) may serve as a quick tool to estimate the stiffness of CNT-based composites in the axial direction when the CNTs are relatively short, while the conventional rule of mixtures (Eq. (11)) can continue to serve in cases when the CNTs are relatively long.

6. Discussions

The effective mechanical properties of carbon nanotube-based composites are evaluated using a 3-D nanoscale RVE based on 3-D elasticity theory and solved by the finite element method. Formulas to extract the material constants from solutions for the RVE under three loading cases are established using the elasticity. An *extended rule of mixtures*, which can be used to estimate the Young's modulus in the axial direction of the RVE and to validate the numerical solutions for short CNTs, is

also derived using the strength of materials theory. Numerical examples using the FEM to evaluate the effective material constants of a CNT-based composites are presented, which demonstrate that the reinforcing capabilities of the CNTs in a matrix are significant. With only about 2% and 5% volume fractions of the CNTs in a matrix, the stiffness of the composite in the CNT axial direction can increase as many as 0.7 and 9.7 times for the cases of short and long CNT fibers, respectively. These simulation results, which are believed to be the first of its kind for CNT-based composites, are consistent with the experimental results reported in the literature (see, e.g. (Schadler et al., 1998; Wagner et al., 1998; Bower et al., 1999; Qian et al., 2000)). The developed extended rule of mixtures is also found to be quite effective in evaluating the stiffness of the CNT-based composites in the CNT axial direction.

Many research issues need to be addressed in the modeling and simulations of CNTs in a matrix material for the development of nanocomposites. Analytical methods and simulation models to extract the mechanical properties of the CNT-based nanocomposites need to be further developed and verified with experimental results. The analytical method and simulation approach developed in this paper are only a preliminary study. Different type of RVEs, load cases and different solution methods should be investigated. Different interface conditions, other than perfect bonding, need to be investigated using different models to more accurately account for the interactions of the CNTs in a matrix material at the nanoscale. Nanoscale interface cracks can be analyzed using simulations to investigate the failure mechanism in nanomaterials. Interactions among a large number of CNTs in a matrix can be simulated if the computing power

is available. Single-walled and multi-walled CNTs as reinforcing fibers in a matrix can be studied by simulations to find out their advantages and disadvantages. Finally, large multiscale simulation models for CNT-based composites, which can link the models at the nano, micro and macro scales, need to be developed, with the help of analytical and experimental work.

The three RVEs proposed in (Liu and Chen, 2002) and shown in Fig. 1 are relatively simple regarding the models and scales. However, this is only the first step toward more sophisticated and large scale simulations of CNT-based composites. As the computing power and confidence in simulations of CNT-based composites increase, large-scale 3-D models containing hundreds or even more CNTs, behaving linearly or nonlinearly, with coatings or of different sizes, distributed evenly or randomly, can be employed to investigate the interactions among the CNTs in a matrix and to evaluate the effective material properties. Other numerical methods can also be attempted for the modeling and simulations of CNT-based composites, which may offer some advantages over the FEM approach. For example, the boundary element method (Liu et al., 2000; Chen and Liu, 2001), accelerated with the fast multipole techniques (see, e.g. (Fu et al., 1998; Nishimura et al., 1999)), and the meshfree methods (Qian et al., 2001) may enable one to model an RVE with thousands of CNTs in a matrix on a desktop computer. Analysis of the CNT-based composites using the boundary element method is already underway and will be reported subsequently.

Acknowledgement

The financial support to the second author (XLC) from the University Research Council at the University of Cincinnati is acknowledged.

References

- Bower, C., Rosen, R., Jin, L., Han, J., et al., 1999. Deformation of carbon nanotubes in nanotube-polymer composites. *Applied Physics Letters* 74 (22), 3317–3319.
- Buongiorno Nardelli, M., Fattebert, J.-L., Orlikowski, D., Roland, C., et al., 2000. Mechanical properties, defects and electronic behavior of carbon nanotubes. *Carbon* 38 (11–12), 1703–1711.
- Chen, X.L., Liu, Y.J., 2001. Multiple-cell modeling of fiber-reinforced composites with the presence of interphases using the boundary element method. *Computational Materials Science* 21 (1), 86–94.
- Cornwell, C.F., Wille, L.T., 1997. Elastic properties of single-walled carbon nanotubes in compression. *Solid State Communications* 101 (8), 555–558.
- Fu, Y., Klimkowski, K.J., Rodin, G.J., Berger, E., et al., 1998. A fast solution method for three-dimensional many-particle problems of linear elasticity. *International Journal for Numerical Methods in Engineering* 42, 1215–1229.
- Gao, G.H., Cagin, T., Goddard, W.A., 1998. Energetics, structure, mechanical and vibrational properties of single-walled carbon nanotubes. *Nanotechnology* 9 (3), 184–191.
- Govindjee, S., Sackman, J.L., 1999. On the use of continuum mechanics to estimate the properties of nanotubes. *Solid State Communications* 110 (4), 227–230.
- Goze, C., Bernier, P., Henrard, L., Vaccarini, L., et al., 1999. Elastic and mechanical properties of carbon nanotubes. *Synthetic Metals* 103 (1–3), 2500–2501.
- Halicoglu, T., 1998. Stress calculations for carbon nanotubes. *Thin Solid Films* 312 (1–2), 11–14.
- Han, J., Globus, A., Jaffe, R., Deardorff, G., 1997. Molecular dynamics simulations of carbon nanotube-based gears. *Nanotechnology* 8 (3), 95–102.
- Hyer, M.W., 1998. *Stress Analysis of Fiber-Reinforced Composite Materials*. McGraw-Hill, Boston.
- Iijima, S., 1991. Helical microtubules of graphitic carbon. *Nature* 354, 568.
- Jia, Z., Wang, Z., Xu, C., Liang, J., et al., 1999. Study on poly(methyl methacrylate)/carbon nanotube composites. *Materials Science and Engineering: A* 271 (1–2), 395–400.
- Kang, J.-W., Hwang, H.-J., 2001. Mechanical deformation study of copper nanowire using atomistic simulation. *Nanotechnology* 12 (3), 295–300.
- Krishnan, A., Dujardin, E., Ebbesen, T.W., Yianilos, P.N., et al., 1998. Young's modulus of single-walled nanotubes. *Physical Review B-Condensed Matter* 58 (20), 14013–14019.
- Liu, Y.J., Chen, X.L., 2002. Modeling and analysis of carbon nanotube-based composites using the FEM and BEM. Submitted to *CMES: Computer Modeling in Engineering and Science*.
- Liu, Y.J., Xu, N., Luo, J.F., 2000. Modeling of interphases in fiber-reinforced composites under transverse loading using the boundary element method. *Journal of Applied Mechanics* 67 (1), 41–49.
- Lu, J.P., 1997. Elastic properties of single and multilayered nanotubes. *Journal of Physics and Chemistry of Solids* 58 (11), 1649–1652.
- Macucci, M., Iannaccone, G., Greer, J., Martorell, J., et al., 2001. Status and perspectives of nanoscale device modelling. *Nanotechnology* 12 (2), 136–142.

- Nemat-Nasser, S., Hori, M., 1999. *Micromechanics: Overall Properties of Heterogeneous Materials*. Elsevier, Amsterdam.
- Nishimura, N., Yoshida, K.-i., Kobayashi, S., 1999. A fast multipole boundary integral equation method for crack problems in 3D. *Engineering Analysis with Boundary Elements* 23, 97–105.
- Qian, D., Dickey, E.C., Andrews, R., Rantell, T., 2000. Load transfer and deformation mechanisms in carbon nanotube-polystyrene composites. *Applied Physics Letters* 76 (20), 2868–2870.
- Qian, D., Liu, W.K., Ruoff, R.S., 2001. Mechanics of C_{60} in nanotubes. *The Journal of Physical Chemistry B* 105 (44), 10753–10758.
- Qian, D., Wagner, G.J., Liu, W.K., Yu, M.-F., et al., 2002. Mechanics of carbon nanotubes. *Applied Mechanics Reviews*, November, to be published.
- Ru, C.Q., 2000. Column buckling of multiwalled carbon nanotubes with interlayer radial displacements. *Physical Review B* 62 (24), 16962–16967.
- Ru, C.Q., 2001. Axially compressed buckling of a doublewalled carbon nanotube embedded in an elastic medium. *Journal of the Mechanics and Physics of Solids* 49 (6), 1265–1279.
- Ruoff, R.S., Lorents, D.C., 1995. Mechanical and thermal properties of carbon nanotubes. *Carbon* 33 (7), 925–930.
- Salvetat, J.P., Bonard, J.M., Thomson, N.H., Kulik, A.J., et al., 1999. Mechanical properties of carbon nanotubes. *Applied Physics A—Materials Science & Processing* 69 (3), 255–260.
- Schadler, L.S., Giannaris, S.C., Ajayan, P.M., 1998. Load transfer in carbon nanotube epoxy composites. *Applied Physics Letters* 73 (26), 3842–3844.
- Sinnott, S.B., Shenderova, O.A., White, C.T., Brenner, D.W., 1998. Mechanical properties of nanotubule fibers and composites determined from theoretical calculations and simulations. *Carbon* 36 (1–2), 1–9.
- Sohlberg, K., Sumpter, B.G., Tuzun, R.E., Noid, D.W., 1998. Continuum methods of mechanics as a simplified approach to structural engineering of nanostructures. *Nanotechnology* 9 (1), 30–36.
- Srivastava, D., Menon, M., Cho, K., 2001. Computational nanotechnology with carbon nanotubes and fullerenes. *Computing in Science and Engineering* 3 (4), 42–55.
- Thostenson, E.T., Ren, Z.F., Chou, T.-W., 2001. Advances in the science and technology of carbon nanotubes and their composites: a review. *Composites Science and Technology* 61, 1899–1912.
- Timoshenko, S.P., Goodier, J.N., 1987. *Theory of Elasticity*. McGraw-Hill, New York.
- Treacy, M.M.J., Ebbesen, T.W., Gibson, J.M., 1996. Exceptionally high Young's modulus observed for individual carbon nanotubes. *Nature* 381 (6584), 678–680.
- Wagner, H.D., Lourie, O., Feldman, Y., Tenne, R., 1998. Stress-induced fragmentation of multiwall carbon nanotubes in a polymer matrix. *Applied Physics Letters* 72 (2), 188–190.
- Wong, E.W., Sheehan, P.E., Lieber, C.M., 1997. Nanobeam mechanics: elasticity, strength, and toughness of nanorods and nanotubes. *Science* 277 (5334), 1971–1975.
- Yao, N., Lordi, V., 1998. Young's modulus of single-walled carbon nanotubes. *Journal of Applied Physics* 84 (4), 1939–1943.